

Cite this: *J. Mater. Chem. C*, 2014, 2, 6773

Nanowires with unusual packing of poly-(3-hexylthiophene)s induced by electric fields

Zhi Ye, Xiubao Yang, Huina Cui and Feng Qiu*

We promote nanowire formation in a thin film of poly(3-hexylthiophene) (P3HT) by applying a strong electric field. Molecular packing in the formed nanowires is surprisingly different from that usually obtained by thermal annealing or from dilute solutions. In the case of electric-field annealing, the P3HT backbones are parallel to the nanowire axis; while in the former cases of thermal annealing, its backbones are perpendicular to the wire axis. Furthermore, this unusual one-dimensional nanowire exhibits improved crystallinity and electric conductivity compared to the corresponding thermally annealed sample. The growth of unusual nanowires is attributed to the introduction of dipolar interactions at the polymer ends by electric field. This kind of nanowire creates effective charge transport pathways along the intrachain route and contributes to the enhanced conductivity of the P3HT films.

Received 2nd April 2014
Accepted 11th June 2014

DOI: 10.1039/c4tc00668b

www.rsc.org/MaterialsC

Introduction

Conjugated polymer is widely regarded as a promising semi-conducting polymer because of its use in field-effect transistors (FETs), biosensors, and solar cells.^{1–4} Among various conjugated polymers, poly(3-hexylthiophene) (P3HT) has attracted more attention for its excellent chemical stability, high performance, and simple preparation techniques.^{4,5} Organized nanostructures of P3HT are mainly obtained by self-assembling from its dilute solutions or by thermal annealing around its crystallization temperature, leading to the formation of one-dimensional (1D) nanowires,⁶ which provide good vertical pathways for charge transport in fabricating vertical-type electronics such as photovoltaic devices.^{7–9} In addition, long nanowires exhibit a low percolation threshold and an excellent mechanical property.¹⁰ Typically, P3HT nanowires can be formed with an average width of ~15 nm and a thickness of 1.6–5 nm, corresponding to one or several P3HT monolayers.^{11,12} The equilibrium anisotropy of its 1D nanostructure is determined by several kinds of interactions such as π - π stacking interactions, hydrophobic interactions between side chains, and interfacial interactions between the solution and polymers. The dominant force of π - π stacking interaction results in P3HT chains preferably packed as 1D nanowires with (010) direction (the π - π stacking direction) parallel to the nanowire axis.^{9,13,14}

Directing nanowire growth with other packing modes (*i.e.*, chain backbones parallel to nanowire axis) has attracted significant attention because the packing of conjugated

polymers within the nanowires determines the charge transport route and transport mechanism.¹⁵ Therefore, it is important to explore a strategy for guiding the assembling process of polymer chains. The self-organized structures of poly(3-alkylthiophene)s are considerably influenced by the length of the alkyl side chains, molecular weight, quality of the solvent, and annealing temperature, resulting in different types of assembled structures such as nanorings and nanobelts.^{12,16,17} Although several useful nanostructures have been obtained, 1D P3HT nanowires preferably packed with polymer chains parallel to the nanowire axis are scarce.¹⁸ Controlling polymer backbone packing direction within nanowires, especially the simultaneous control of polymer chain alignment and high crystallinity, remains a challenge.

Electric fields are widely used to induce the assembling of colloidal particles into chains by employing an extra force because of dipolar interactions among the particles.^{19–22} In the last decade, particles that can be manipulated under electric fields have been extended to different shapes such as polyhedral particles, rod-like particles and chiral colloidal clusters.^{19,23–25} Similarly, rod-like conjugated polymers also have an induced dipolar for charges that can migrate along the backbones within a conjugation length, which was suggested to be 20–30 monomers (7.8–11.7 nm) in P3HT.^{26–28} Chen *et al.* used an electric field of 0.6 V μm^{-1} normal to the film surface during solvent-drying, and found that the crystallinity of the P3HT/PCBM film enhanced slightly. In addition, the width of the crystalline fibrils increased and amorphous boundaries decreased during the electric field treatment.²⁹ Recently, Lee *et al.* applied an electric field of 0.2 V μm^{-1} on P3HT thin film with the field along the in-plane direction. They found that the crystalline domain size increased by 13.4% after the application of the

State Key Laboratory of Molecular Engineering of Polymers, Department of Macromolecular Science, Fudan University, Shanghai 200433, China. E-mail: fengqiu@fudan.edu.cn

electric field.³⁰ These reports prove the evident effects of electric field on conjugated polymer organization. However, the assembling of polymer chains induced by dipolar interactions was not reported in these studies. A possible reason is that the dipolar moment of conjugated polymers is too weak when compared to that of the particles. To maximize the electrostatic force between the chain ends, an electric field as high as $30 \text{ V } \mu\text{m}^{-1}$ on P3HT film was built in the present work by employing an insulated layer such as thermal-growth SiO_2 layer, which has a dielectric breakdown strength of $10^3 \text{ V } \mu\text{m}^{-1}$.³¹ Here, we focus on the packing behavior of rigid P3HT chains under strong electric fields and found that the polymer chains can assemble into nanowires with their backbones parallel to the wire axis, which is in contrast to the expected molecular packing formed in nanowires in the absence of an electric field (with polymer backbones perpendicular to the wire axis). In addition, these long nanowires can form a 3D connecting network after electric-field annealing. We also observe individual P3HT chains packing in single nanowires with perfect order. These unusual nanowires have exhibited excellent crystallinity and improved electrical properties.

Results and discussion

A P3HT film with the thickness varying from 30 nm to 50 nm was prepared by spin coating its chloroform solution onto an n-type Si substrate covered with an electrically insulating layer of 300 nm thick SiO_2 . It is believed that the SiO_2 layer can improve the maximum electric field strength that can be applied for its high breakthrough voltage. In this manner, the hybrid layer, composed of P3HT thin film and thin SiO_2 layer, could bear a high field vertical to the surface before breaking through, despite of the conductive layer of the P3HT thin film. After the removal of the remaining solvent in vacuum, the film was covered with an FTO glass as a top electrode, leaving an air gap of 200 nm from the bottom electrode. A hot stage was placed to assist chain movement by heating. This setup (Fig. 1) was heated to a temperature of $170 \text{ }^\circ\text{C}$ and a voltage of 52 V was immediately applied to the two plates, resulting in an electric field of $30 \text{ V } \mu\text{m}^{-1}$ on the polymer layer, which is several orders of magnitude higher than most studies investigating particle assembly. Leak current was monitored by a multisource measurement with a value ranging from 10^{-2} to $10^{-1} \text{ } \mu\text{A}$. After

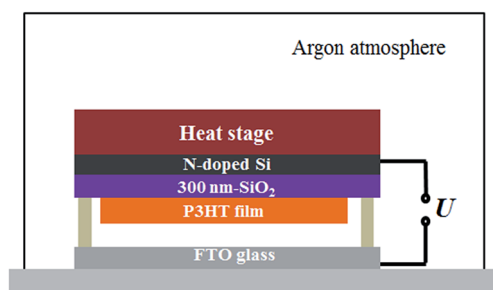


Fig. 1 Schematic representation of the experimental setup and procedure for processing poly(3-hexylthiophene) into nanowires.

an electric field was applied for several minutes to several hours, the setup was cooled to room temperature in argon before the electric field was removed.

Morphologies

Fig. 2 shows the surface topography image of the P3HT films measured by AFM measurement with tapping mode. AFM tapping images of the thermally-annealed film (Fig. 2a) showed featureless morphology at $170 \text{ }^\circ\text{C}$ or formed grain-like crystallites of 100–200 nm in length and 15–25 nm in width at higher temperature (*i.e.* $200 \text{ }^\circ\text{C}$ as shown in Fig. 2b). In the absence of external constraints, π - π interaction between aromatic backbones is the dominant driving force for polymer chain assembling. Through one-dimensional (1D) heterogeneous nucleation, P3HT polymers linearly grow to 1D nanowires with their growth direction coinciding with the π - π stacking direction. Thus, the thermally-annealed nanowires have the same width as the chain contour length when the polymer molecular weight is not very high.^{13,32,33} Fig. 2c and d illustrate the morphologies of the P3HT films under an electric field for 30 min and 8 h, respectively. Both the AFM tapping and phase image clearly show nanowires distributing in the film on the substrate. With electric field annealing for 30 min, the film becomes rough with a height difference of 10–20 nm. High density nanowires are clearly identified in the phase image because it visualizes the hard-soft contrast of the crystalline-amorphous areas in the semicrystalline P3HT. The cross-sectional line profiles obtained across the height image of Fig. 2e show the growth of the wire width of $\sim 40 \text{ nm}$ and a

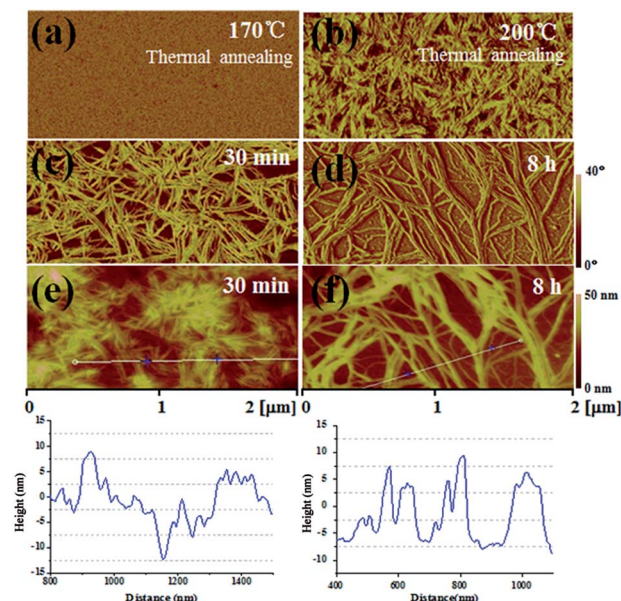


Fig. 2 Representative P3HT nanowires formed under electric fields *via* AFM phase and height images. Phase images of thermally-annealed film at (a) $170 \text{ }^\circ\text{C}$ and (b) $200 \text{ }^\circ\text{C}$. The electric field strength is $30 \text{ V } \mu\text{m}^{-1}$ and the annealed time is (c) 30 min, (d) 8 h; (e) and (f) are the corresponding height images of (c) and (d), respectively. The bottom of the AFM height images are the cross-sectional line profile of the nanowires. For all the images, the scanning size is $2 \times 2 \text{ } \mu\text{m}^2$.

height of ~ 8 nm in average. After increasing the field-annealing time to 8 h (Fig. 2d and f), the density of the nanowires decreased and the nanowires grew wider to ~ 60 nm in average.

AFM height images prove that the assembly in P3HT film displays an interconnecting network consisting of randomly connected nanowires, as shown in Fig. 3. The vertical positions of the wire surfaces disperse from -25 nm to 30 nm on the substrate, indicating that the nanowires formed a 3D network. The length of an individual nanowire is over 10 micrometers. 3D connecting structure could reduce grain boundaries between the neighboring wires and reduce the scatter of charge carriers at the inter-wire sites.¹⁰ Thus, this kind of structure is believed to be useful for vertical-type electronics, in which charges migrate mainly normal to film surface direction.³⁴

The fluctuation of film surface appears to increase when an electric field was applied, as observed from the AFM height images. By comparing the roughness of the films with and without an electric field, it was found that the surface roughness of the film increased from ~ 2 nm (RMS) for the thermally annealed sample to a significantly larger roughness of 16 nm for the electric-field annealed sample. The increased roughness is attributed to the electrohydrodynamic instabilities at polymer liquid–air interfaces induced by an electric field.³⁵ However, it is not easy to generate deep instabilities (*i.e.* pillars span the two parallel electrodes) in this experimental condition because of the high viscosity of the stiff backbone of conjugated polymers.^{36,37}

Structural characterization of the nanowires

HRTEM is a useful tool to directly provide the detailed packing of polymer chains at molecular scale. We performed TEM and HRTEM to further investigate the nanowires with an electric field treatment at an early stage. The film was transferred to a copper grid in dilute HF solution for TEM characterizations. A wire-like P3HT film with distinct dark and bright lines is shown in Fig. 4a, which was treated under an electric field for 5 min. Its

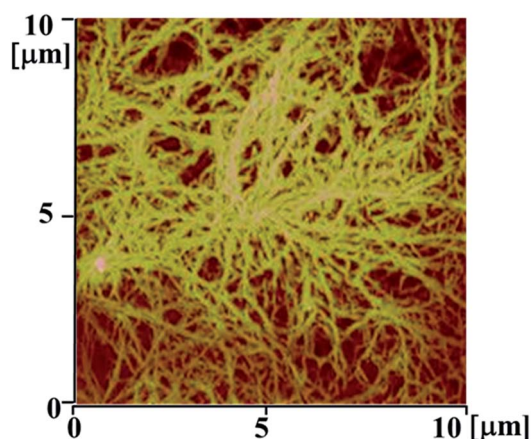


Fig. 3 AFM height image of electric-field treated film for 11 h. The electric field strength is $30 \text{ V } \mu\text{m}^{-1}$ and the annealing temperature is 170°C . P3HT nanowires form 3D connecting network. An individual nanowire in the image has an average length of over $10 \mu\text{m}$ and an average width of over 100 nm . The height scale of the height image is 100 nm .

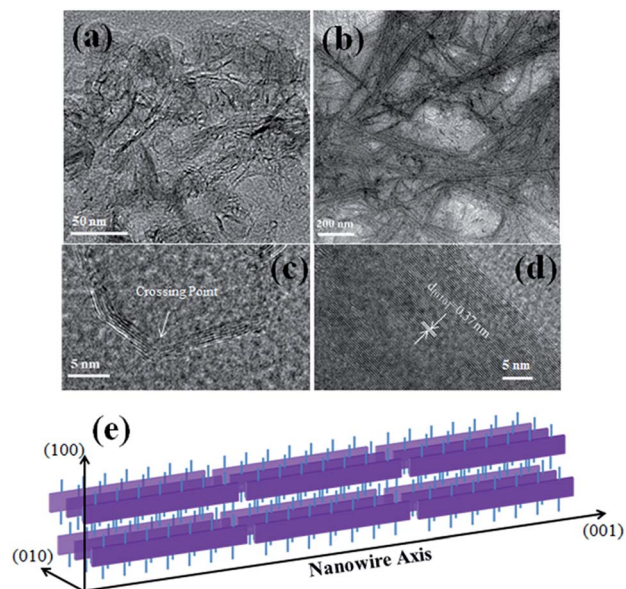


Fig. 4 Representative TEM images of P3HT wires at 170°C under an electric field for (a) 5 min and (b) 30 min. (c) and (d) are the corresponding HRTEM images, respectively. Clear stripes indicate excellent crystalline structures of the nanowires. (e) Schematic representing P3HT chain packing within an individual nanowire.

corresponding HRTEM pattern (Fig. 4c) reveals that the wire-like P3HT film actually consists of randomly distributed crystalline nanowire with a width of $1\text{--}3 \text{ nm}$. The nanowires form in a circle composed of connected P3HT chains bridged head to end and the nanocrystalline lamellae are clear in the HRTEM image. The extended length of the nanocrystalline is about 13 nm (Fig. 4c), corresponding to a single chain length of the P3HT (M_n of P3HT measured by GPC is actually over estimated by 70%). Grain boundaries between two adjacent nanocrystalline lamellae show an angle in the range of $20\text{--}60^\circ$. The reasonably smooth connection indicates that there may be an end-to-end interaction to organize the assembled P3HT chains. For longer time treatment (*i.e.* 30 min), the nanowire grew to $5\text{--}30 \text{ nm}$ in width and over one micrometer in length, as shown in Fig. 4b and d. The P3HT chains in the film aggregated into a network in the form of densely connecting nanowires, which is consistent with the corresponding AFM images. With increasing electric field-annealing time, the nanowire became more stiff, the grain boundary angle decreased to about 0° and the cross point became undistinguished. Both the HRTEM images identify the “edge-on” orientation of the crystallites with periodic lamellar pattern corresponding to a $\pi\text{--}\pi$ stacking distance of 0.37 nm . The clear HRTEM image also shows excellent crystallinity of the P3HT nanowires because the HRTEM image is essentially a 2D projection from the diffraction of the 3D crystalline structure.

Based on the abovementioned HRTEM and AFM images, we propose the electric field induced P3HT nanowire packing structure, as shown in Fig. 4e. Within a single P3HT nanowire, the P3HT backbones are parallel to nanowire axis, which is significantly different from the self-assembled nanowires of P3HT by thermal annealing or solvent vapor annealing.^{12,14} This

kind of unusual anisotropic packing has also been found in BBL nanobelts, and it is believed that an extraordinary strength of intermolecular interactions originates from the rigid and planar backbone of BBL chain.³⁸ Obviously, the nanowires of P3HT in our experiment have a more ordered chain packing than the BBL nanobelts, judging from the SAED results. The TEM micrograph for samples in the absence of applied field proves that the thermally annealed film consists of both wire structure and amorphous region. Complementary HRTEM examinations reveal no periodic fringed pattern within these wires. HRTEM image of polymer chain packing is essentially the reciprocal space of diffraction pattern in P3HT single crystalline structures, and therefore the crystallization of nanowire has a significant affect on the resolution of its HRTEM images. It implies that the P3HT nanowires prepared by thermal annealing have a lower degree of crystallization than that obtained by electric-field annealing. In fact, to the best of our knowledge, HRTEM image of P3HT nanowires by thermal annealing or in solution have not been reported because of its semi-crystalline structure.

Other field-annealing temperatures were also investigated in the present study. At temperatures lower than 160 °C or higher than 210 °C, nanowires were not found in their TEM images. However, when the electric field-annealing temperature was 200 °C, numerous looped nanowires (nanorings) were observed with diameter ranging from 10 nm to 30 nm and width ranging from 2 nm to 5 nm, as shown in Fig. 5a. The corresponding HRTEM image (Fig. 5c) shows the P3HT chains packing with the polymer backbones parallel to the long axis of the nanorings. Interestingly, a part of the nanowire is actually half-looping, leaving a head-to-end distance of about 2 nm, as shown in Fig. 5d. Compared to rod-like polymer chains in Fig. 4c with a lower annealing temperature of 170 °C, the polymer chains

appear flexible and a part of chains can bend over 90°. This indicates that the annealing temperature exerts a profound influence on the stiffness of the polymer chains. At higher temperatures, polymer chains are easy to bend, while at lower temperatures, polymer chains are stiff and rod-like. Bright diffraction rings are observed from the SAED pattern of the field-treated film (Fig. 5b), identifying the existence of the crystalline (020) plane with a π - π stacking distance of 0.37 nm. Nanorings have also been found in our previous reports, referring to the self-assembly of poly(3-alkylthiophene) diblock copolymer in solution.¹⁶ Obviously, polymer chain packing behavior in the nanowires is different from that in diblock copolymer formed nanowires, indicating a different process of nanoring formation under electric field.

The impact of electric fields on structural changes was investigated by UV-vis absorption spectra, which are correlated with the structural properties of the thin films of the crystalline nanowires.^{39,40} For the thermally annealed film, the 0-0 contribution at 610 nm and the dominating 0-1 contribution at 560 nm were visible from the black curve in Fig. 6. The ratio of 0-0/0-1 absorbance peaks is about 0.8, indicating a significant interchain coupling (H-aggregate).⁴¹ For the films treated by electric-field annealing for 30 min, the 0-0/0-1 intensity ratio shows an increase, implying a larger conjugation length within the polymer chain.²⁸ Furthermore, both 0-0/0-1 absorbance peaks exhibit red shifts of \sim 10 nm when the P3HT films went from thermal annealing to the electric-field annealing. The increased 0-1 intensity is because of the ordered stacking of the polymer backbones in the films, and the increase in 0-0 intensity is correlated with the degree of interchain order, which indicates that the crystallinity of the electric field-treated film is enhanced.^{5,42}

Mechanism of anisotropic nanowires with high crystallinity

Apparently, the electric field can assist the packing of P3HT chains. In fact, electric fields are widely used to enable the manipulation of the dipolar interaction between the spherical colloids, leading to long colloid chains along the electric field direction, while short-range attractions such as van der Waal's

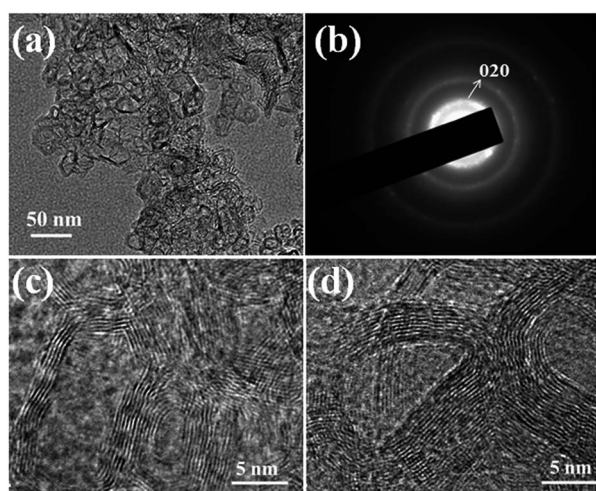


Fig. 5 (a) Representative TEM image of P3HT film under an electric field for 5 min. Nanorings were observed with a diameter of 15–50 nm and a width of 1–10 nm. (b) Corresponding SAED pattern of the TEM image. (c) and (d) HRTEM images showing the detail of chain packing in the nanorings. Closed rings (c) and half-closed rings (d) are found with polymer backbones parallel to the circumferences of the nanorings.

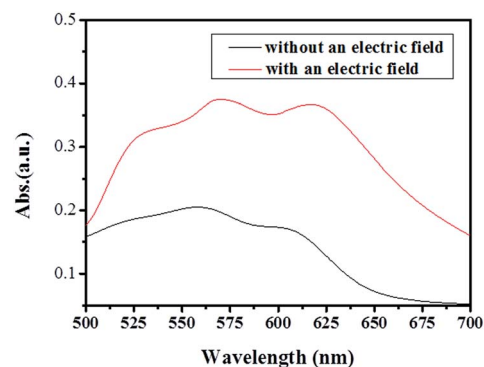


Fig. 6 Absorption spectra of the P3HT thin film treated by thermal annealing (black line) and by an electric field of 30 V μm^{-1} (red line). All the films were annealed at 170 °C for 30 min.

forces keep the assembled colloids from dispersing. We believe a similar mechanism exists in the electric field induced P3HT nanowires. In thermal annealing, both π - π stacking and van der Waal's interaction govern the self-assembly of P3HT, and π - π stacking force dominates the self-assembled behavior, resulting in a polymer chain perpendicular to the nanowire axis.^{18,38} Charge could delocalize within a conjugation length along the backbone but are laterally confined in the polymer chain, generating an intrinsic dipole moment under electric field.^{15,28,43,44} For a ribbon like ladder-type polymer, the chain ends determine the effective conjugation length of the polymer.⁴⁵ However, in other conjugated polymers such as P3HT, the effective conjugation is often reduced by structural defects or torsional disorder. Thus, for low molecular weight P3HT, the conjugation length corresponds to the length of the polymer chain. For the 11–19 kg mol⁻¹ P3HT, it was proven that the conjugation length was about half of the polymer chain length using the MALDI-TOF MS measurements.⁴⁶ The conjugation length of P3HT was also suggested to be 20–30 monomers (7.8–11.7 nm), according to the calculations reported by Clark.²⁷ The conjugation length in our experiment should be even larger because of an increased 0–0/0–1 ratio. Based on these facts, it is reasonable to deduce that the entire P3HT chain may consist of only one or two conjugation lengths. Therefore, we believe there is a large probability of the distribution of dipole charges in the chain ends.

Fig. 7 depicts the proposed process of nanowire formation under an electric field. In an electric field normal to the film surface, each P3HT chain bears an induced dipole moment along the backbone direction. After heating to above their glass transition temperature, the P3HT chains start to move and self-assemble into end-connecting nanowire. The main driving force in this process is the dipolar interactions between the chain ends. For polymer bending at a high temperature (*i.e.* 200 °C), the narrow nanowires could orient themselves as a hoop and nanorings form. This step of assembling, in our observation of the HRTEM experiments, takes less than 5 min, which may be attributed to the long-range electrostatic interaction of the dipoles. The next step of polymer assembling is the widening of the nanowires, which is mainly driven by π - π interaction between aromatic backbones. In this step, the nanowires could grow up to 100 nm in width and over 10 μ m in length after electric-field annealing for 11 h.

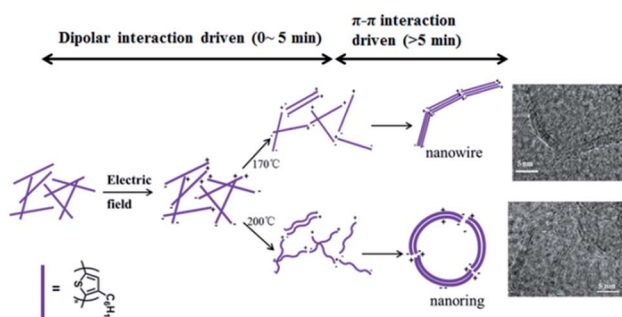


Fig. 7 Schematic diagram of the possible mechanisms for P3HT to assemble into nanowires or nanorings under an electric field.

We believe that heating at high temperature (170 °C) provides the thermal energy required to bend the otherwise straight chain backbones under an electric field. Initially, it is possible that three or more slightly bending chains are connected by dipole interactions, forming the inner core of the hoops or nanorings. Later, increasing numbers of chains join this process and finally develop into hoops and nanorings. A careful inspection shows that each chain backbone in the fibrils is only slightly bent, although the fibrils form hoops and nanorings. The large bending of the fibrils is due to an accumulative effect.

The crystallinity of the P3HT films was characterized by X-ray grazing incidence diffraction (GIXRD) measurements using synchrotron X-ray radiation. Two films spin-coated from a chloroform solution were prepared with a thickness of 40 nm, as determined by AFM measurement. The two films were annealed at 170 °C with and without electric field (30V μ m⁻¹) for 30 min, respectively. The nanocrystalline alignment was investigated using 2D GIXRD measurement, which probes all the crystalline plane orientations in the thin film. Both the 170 °C annealed films with and without the electric field show an arc pattern (*h*00) along the Q_z direction (Fig. 8c and d), which indicates that the chains in the nanocrystallines are packing in “edge on” configuration through the process of electric field annealing. Electric field illustrates that the two films exhibit a crystalline structure with the “edge on” configuration. Thus, the strong diffraction and the appeared second-order diffraction (Fig. 8d) suggest an enhancement in the crystallinity of the film under an electric field. The high crystallinity of the film is also in agreement with the HRTEM results from the nanowires.

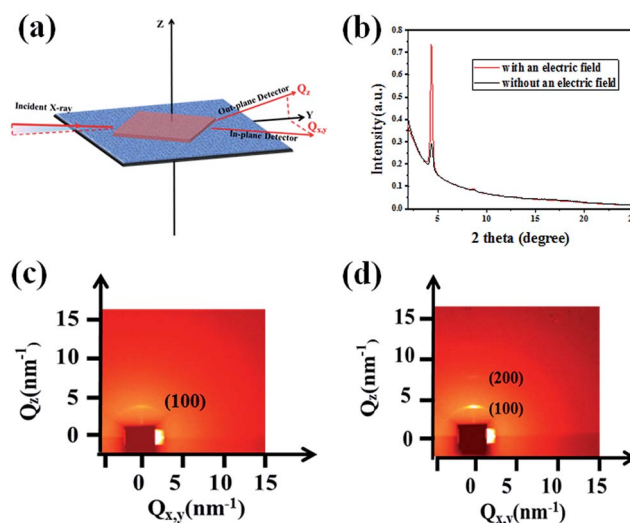


Fig. 8 X-ray grazing incidence diffraction (GIXRD) experiment of the P3HT films. (a) Schematic illustration of the synchrotron GIXRD measurement for the P3HT films on a Si/SiO₂ substrate where the incidence angle of the synchrotron X-ray beam is 0.15°. (b) Out-of-plane X-ray diffraction pattern of the P3HT films with thermal annealing at 170 °C for 30 min (black line) with electric-field annealing at 170 °C for 30 min (red line). (c) and (d) 2D GIXRD images of the P3HT thin films without and with electric-field annealing. Both (100) and (200) diffractions can be observed for the electric-field annealed film in the out-of-plane (Q_z) direction.

1D GIXRD pattern along the Q_z direction quantitatively recorded the enhanced crystallinity of the film. For the thermally annealed film, the out-of-plane diffraction shows a weak reflection at an interlayer d -spacing of 16.36 Å ($2\theta = 4.35^\circ$). The interlayer spacing is consistent with the reported structural model, where the side chains of P3HT are interdigitated with each other.⁴⁷ After an applied electric field, the intensity of the peak increases to about 4.8 folds at (100) reflection (Fig. 8b). The same (100) position of 2θ indicates that the interlayer spacing does not change with and without the electric field. Crystalline size along the direction normal to the surface can be calculated by Scherrer equation, in which the average crystalline size in (100) direction is inversely proportional to full width at half maximum (FWHM) of the (100) peak.^{29,30} As shown in Fig. 8b, the FWHM of (100) reflection decreases from 0.28° to 0.18° after electric-field annealing. This indicates that the crystalline domains are 55.6% larger than those treated with thermal annealing in the absence of an electric field. Therefore, it is reasonable to deduce that the crystallinity of electric-field annealed film is three times higher than its thermal annealed counterparts by comparing (100) peak area in 1D-GIXRD results.

GIXRD measurements proved the “edge on” configuration of the crystalline packing on the substrate. In addition, the reorientation of P3HT nanocrystallites under an electric field was not found in our experiment. This appears to be different from the aligning of inorganic nanorods or conjugated polymers in a solution, which can stand perpendicular to the underlying substrate.^{26,48,49} Nanorods tend to align the induced dipole moment along the electric field. The absence of this kind of P3HT reorientation may be attributed to the weak dipole moment of conjugated polymer and unfavorable interfacial interactions between the polymer chains and the SiO_2/Si

substrate when the long chains stand normal to the film surface.²⁸

To achieve chain packing with high crystallinity, polymers have to overcome several energy barriers, which are caused by the rearrangement of chain conformations. Thus, the ordered arrangement of polymer chains have lower energy barriers and promote the crystallinity of polymers during polymer crystallization.^{18,50,51} We used this hypothesis to explain the enhancement of crystallinity in P3HT films treated by electric fields. The main driving force of P3HT crystallization is considered to be π - π stacking interactions for thermal annealing or in a solution, resulting in a crystallinity of 10% to 20%.^{13,33} Most of the polymer chains in the P3HT film are randomly distributed around the crystalline phase. A key step to help crystallization is to assemble the polymers in an ordered state by further short-range chain interactions.⁵² Under a strong electric field, an extra force from the dipolar interactions connects the P3HT chains end by end, thus assisting the arrangement of the disordered chains in an amorphous region. As a result, an electric field may facilitate P3HT crystallization by promoting chain arrangement, resulting to an enhanced crystallinity of the P3HT films.

Electrical properties

It is interesting to compare the electrical property of the electric-field annealed P3HT films with that of the thermally annealed films. The measured current for the spin-coated film increased up to three times during thermal annealing for 30 min at 170°C without electric field (Fig. 9). With an electric field annealing of $30\text{ V }\mu\text{m}^{-1}$ for 30 min, the conductivity of P3HT increases substantially with more than one order-of-magnitude (from $0.05\text{ }\mu\text{A}$ to $1.2\text{ }\mu\text{A}$) higher. The improvement in conductivity is because of a combination of increased crystallinity and the preferred orientation of P3HT chains in the nanowires. It has been suggested that the π - π stacking of the conjugated polymer chains allows hole delocalization between the chains and provides a transport route along the interchain direction, rather than only transport along the intrachain (backbone) direction in amorphous regions.¹⁵ Thus, the increased proportion of crystalline area facilitates charge transport in the P3HT films. Among the two transport processes, charge transport along the backbone is significantly easier than that along the π - π stacking direction, indicating that the P3HT nanowires with backbones parallel to the wire axis are more suitable for charge transport than the P3HT nanowires with π - π stacking parallel to the wire axis.⁵³

Conclusions

In summary, we have devised a simple and effective route to control the hierarchically structured assembly of P3HT nanowires with polymer backbones parallel to the nanowire axis. It offers a complementary use of electric fields to obtain anisotropic nanostructures by utilizing dipolar attractions between the polymer ends. The resultant preferential end-to-end attachment within nanowires formed a connecting network with increased crystallinity as well as enhanced conductivity.

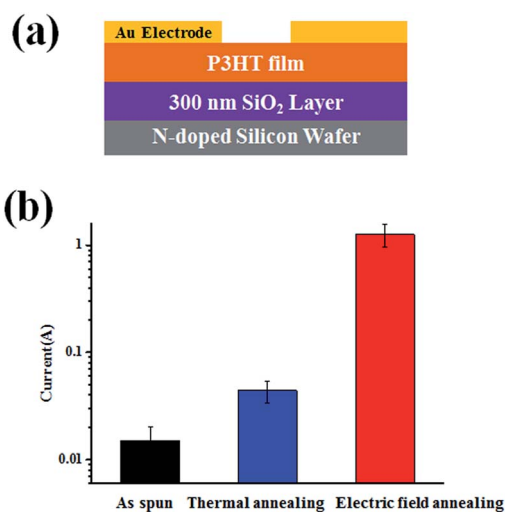


Fig. 9 Electrical conductivity of the spin-coated P3HT films without annealing (black), with thermal annealing at 170°C for 30 min (blue) and with electric-field annealing at 170°C for 30 min (red). (a) Schematic of the electrical conductivity measurement; two probe Au electrodes were directly deposited on the film. (b) Current measurements for P3HT thin film with different treatments at an applied voltage of 10 V.

Different from most inorganic nanorods or conjugated polymers in a solution, we have not observed P3HT chain reorientation normal to the film surface, and the chains remain in an "edge on" orientation throughout electric-field annealing. On extrapolation to the use of electric field adjusting P3HT chain self-assembly, the special molecular packing of wires on nanoscale may provide a viable extension to highly efficient photovoltaic devices and field-effect transistors.

Experimental section

Materials

Highly doped n-type Si substrates coated by a layer of thermally-grown SiO₂ (*i.e.*, ~300 nm thick) was purchased from Materials Technology Company. Silicon oxide colloids with a diameter of 200 nm were purchased from Sigma-Aldrich. Poly(3-hexylthiophene) (P3HT) was synthesized by a modified Grignard method in our lab according to our previous report with molecular weights of 11 kg mol⁻¹, which is determined by gel permeation chromatography (GPC) using a Agilent 1100 system (calibration: polystyrene standards). Differential scanning calorimetry (DSC) was performed using Q2000 at a heating and cooling rate of 10 °C min⁻¹ under an N₂ flow. Crystallization temperature and melt temperature were 185 °C and 219 °C, respectively. Chloroform and hydrofluoric acid (HF) were purchased from Sigma-Aldrich and used without further purifications. The fluorine-doped tin oxide (FTO)-coated glass slide with a resistance of about 20 Ω was used as the transparent electrode on top.

Experimental procedure

SiO₂/Si substrates were sequentially cleaned by ultrasonication in acetone, isopropyl alcohol, followed by Piranha solution (H₂SO₄-H₂O₂ = 3 : 1) and deionized water. P3HT was dissolved in chloroform at 90 °C and purified with a 0.22 μm PTFE filter to yield a ~5 mg ml⁻¹ P3HT/chloroform solution. The P3HT solution was then spin coated on the SiO₂/Si substrates at 3000 rpm for 60 s, resulting in a film with a thickness of 30–50 nm. The FTO-coated glass slides were cleaned by washing in an ultrasonic bath with acetone and isopropanol, and exposing them to oxygen plasma for 15 min. A small air gap of typically 200 nm between the two parallel plates was created by spreading silicon oxide colloids onto the film before mounting on the top electrode. The plate capacitor was connected to a power supply (Keithley 2400 DC), and a vertical electric field was then applied on the P3HT film. Leak current was monitored by a multisource measurement. Both the two electrodes were contacted using conductive carbon paint. The setup was placed on a hot stage with an accuracy of 1 °C and heated to the temperature of 170–200 °C. To prevent the P3HT film from oxidation, an argon flow was conducted to keep the film in inert atmospheric conditions.

Characterization

All 2D X-ray grazing incidence diffraction (GIXRD) pattern and 1D GIXRD pattern of P3HT were obtained using a wavelength of λ = 0.124 nm at BL14B1 of Shanghai Synchrotron Radiation Facility. The exposure time was 50 seconds for 2D pictures. For

1D GIXRD measurement, the exposure time was 1 second and the scan step was 0.05°. The incidence angle was 0.15° in our measurements. The morphologies of the films were characterized on a Bruker Multimode AFM Nanoscope IV with the tapping mode. For the characterizations of high-resolution transmission electron microscope (HRTEM), a dilute HF aqueous solution was used to float off the film from SiO₂/Si substrate, and then the film was transferred to a copper grid. The film was characterized using a JEOL JEM-2100F field-emission transmission electron microscope with a working voltage of 200 kV. To minimize the burn effect of electron beam and to obtain clear HRTEM images, we reduced the operating voltage to 100–150 kV and employed the exposure time for the thin film as short as possible. Absorption spectra of the P3HT films were measured with a Lambda 750 UV-vis spectrophotometer in ambient environment.

Conductivity measurement

Current measurements were performed at a constant applied voltage on the nanowires formed on the Si/SiO₂ substrate. Two 4 mm-length Au electrodes separated by a 100 μm gap were thermally deposited on the films. The electrodes were prepared by depositing 60 nm Au on the P3HT thin films through a mask by thermal evaporation at a vacuum of 2 × 10⁻⁶ mbar. The electrical characterization was measured using a Keithley 6913 power supply in a glove box.

Acknowledgements

We gratefully acknowledge the support from the BL14B1 beamline of Shanghai Synchrotron Radiation Facility of China for the characterization of grazing-incidence X-ray diffraction (GIXRD). We also gratefully acknowledge the financial support from the National Basic Research Program of China (Grant no. 2011CB605700) and the National Natural Science Foundation of China (Grant no. 21320102005).

Notes and references

- 1 H. Sirringhaus, N. Tessler and R. H. Friend, *Science*, 1998, **280**, 1741–1744.
- 2 J. Janata and M. Josowicz, *Nat. Mater.*, 2003, **2**, 19–24.
- 3 M. He, W. Han, J. Ge, W. J. Yu, Y. L. Yang, F. Qiu and Z. Q. Lin, *Nanoscale*, 2011, **3**, 3159–3163.
- 4 M. He, W. Han, J. Ge, Y. L. Yang, F. Qiu and Z. Q. Lin, *Energy Environ. Sci.*, 2011, **4**, 2894–2902.
- 5 J. Ge, M. He, F. Qiu and Y. L. Yang, *Macromolecules*, 2010, **43**, 6422–6428.
- 6 M. Brinkmann and P. Rannou, *Macromolecules*, 2009, **42**, 1125–1130.
- 7 H. Xin, F. S. Kim and S. A. Jenekhe, *J. Am. Chem. Soc.*, 2008, **130**, 5424.
- 8 J. S. Kim, J. H. Lee, J. H. Park, C. Shim, M. Sim and K. Cho, *Adv. Funct. Mater.*, 2011, **21**, 480–486.
- 9 A. L. Briseno, S. C. B. Mannsfeld, S. A. Jenekhe, Z. Bao and Y. N. Xia, *Mater. Today*, 2008, **11**, 38–47.

- 10 S. B. Jo, W. H. Lee, L. Z. Qiu and K. Cho, *J. Mater. Chem.*, 2012, **22**, 4244–4260.
- 11 A. Zen, M. Saphiannikova, D. Neher, J. Grenzer, S. Grigorian, U. Pietsch, U. Asawapirom, S. Janietz, U. Scherf, I. Lieberwirth and G. Wegner, *Macromolecules*, 2006, **39**, 2162–2171.
- 12 J. H. Liu, M. Arif, J. H. Zou, S. I. Khondaker and L. Zhai, *Macromolecules*, 2009, **42**, 9390–9393.
- 13 C. Melis, L. Colombo and A. Mattoni, *J. Phys. Chem. C*, 2011, **115**, 576–581.
- 14 S. Hugger, R. Thomann, T. Heinzl and T. Thurn-Albrecht, *Colloid Polym. Sci.*, 2004, **282**, 932–938.
- 15 R. A. Street, J. E. Northrup and A. Salleo, *Phys. Rev. B: Condens. Matter Mater. Phys.*, 2005, **71**, 165202.
- 16 M. He, L. Zhao, J. Wang, W. Han, Y. L. Yang, F. Qiu and Z. Q. Lin, *ACS Nano*, 2010, **4**, 3241–3247.
- 17 F. S. Kim, G. Q. Ren and S. A. Jenekhe, *Chem. Mater.*, 2011, **23**, 682–732.
- 18 J. A. Lim, F. Liu, S. Ferdous, M. Muthukumar and A. L. Briseno, *Mater. Today*, 2010, **13**, 14–24.
- 19 N. Yanai, M. Sindoro, J. Yan and S. Granick, *J. Am. Chem. Soc.*, 2013, **135**, 34–37.
- 20 M. E. Leunissen, H. R. Vutukuri and A. van Blaaderen, *Adv. Mater.*, 2009, **21**, 3116.
- 21 H. R. Vutukuri, A. F. Demirors, B. Peng, P. D. J. van Oostrum, A. Imhof and A. van Blaaderen, *Angew. Chem., Int. Ed.*, 2012, **51**, 11249–11253.
- 22 A. Yethiraj and A. van Blaaderen, *Nature*, 2003, **421**, 513–517.
- 23 D. Zerrouki, J. Baudry, D. Pine, P. Chaikin and J. Bibette, *Nature*, 2008, **455**, 380–382.
- 24 G. J. Vroege and H. N. W. Lekkerkerker, *Rep. Prog. Phys.*, 1992, **55**, 1241–1309.
- 25 Y. J. Min, M. Akbulut, K. Kristiansen, Y. Golan and J. Israelachvili, *Nat. Mater.*, 2008, **7**, 527–538.
- 26 W. S. Chang, S. Link, A. Yethiraj and P. F. Barbara, *J. Phys. Chem. B*, 2008, **112**, 448–453.
- 27 J. Clark, C. Silva, R. H. Friend and F. C. Spano, *Phys. Rev. Lett.*, 2007, **98**, 206406.
- 28 H. L. Cheng, J. W. Lin, M. F. Jang, F. C. Wu, W. Y. Chou, M. H. Chang and C. H. Chao, *Macromolecules*, 2009, **42**, 8251–8259.
- 29 C. C. Lin, Y. Y. Lin, S. S. Li, C. C. Yu, C. L. Huang, S. H. Lee, C. H. Du, J. J. Lee, H. L. Chen and C. W. Chen, *Energy Environ. Sci.*, 2011, **4**, 2134–2139.
- 30 S. W. Lee, C. H. Kim, S. G. Lee, J. H. Jeong, J. H. Choi and E. S. Lee, *Electron. Mater. Lett.*, 2013, **9**, 471–476.
- 31 K. V. Shcheglov, C. M. Yang, K. J. Vahala and H. A. Atwater, *Appl. Phys. Lett.*, 1995, **66**, 745–747.
- 32 R. J. Kline, M. D. McGehee, E. N. Kadnikova, J. S. Liu, J. M. J. Frechet and M. F. Toney, *Macromolecules*, 2005, **38**, 3312–3319.
- 33 S. Malik and A. K. Nandi, *J. Polym. Sci., Part B: Polym. Phys.*, 2002, **40**, 2073–2085.
- 34 G. M. Newbloom, K. M. Weigandt and D. C. Pozzo, *Macromolecules*, 2012, **45**, 3452–3462.
- 35 E. Schaffer, T. Thurn-Albrecht, T. P. Russell and U. Steiner, *Nature*, 2000, **403**, 874–877.
- 36 F. A. de Castro, F. Nuesch, C. Walder and R. Hany, *J. Nanomater.*, 2012, **2012**, 478296.
- 37 D. R. Barbero and U. Steiner, *Phys. Rev. Lett.*, 2009, **102**, 248303.
- 38 A. L. Briseno, S. C. B. Mannsfeld, P. J. Shamberger, F. S. Ohuchi, Z. N. Bao, S. A. Jenekhe and Y. N. Xia, *Chem. Mater.*, 2008, **20**, 4712–4719.
- 39 L. Hartmann, K. Tremel, S. Uttiya, E. Crossland, S. Ludwigs, N. Kayunkid, C. Vergnat and M. Brinkmann, *Adv. Funct. Mater.*, 2011, **21**, 4047–4057.
- 40 J. Liu, Y. Sun, X. Gao, R. Xing, L. Zheng, S. Wu, Y. Geng and Y. Han, *Langmuir*, 2011, **27**, 4212–4219.
- 41 E. T. Niles, J. D. Roehling, H. Yamagata, A. J. Wise, F. C. Spano, A. J. Moule and J. K. Grey, *J. Phys. Chem. Lett.*, 2012, **3**, 259–263.
- 42 R. J. Kline, M. D. McGehee and M. F. Toney, *Nat. Mater.*, 2006, **5**, 222–228.
- 43 F. Schindler, J. M. Lupton, J. Muller, J. Feldmann and U. Scherf, *Nat. Mater.*, 2006, **5**, 141–146.
- 44 A. Salleo, T. W. Chen, A. R. Volkel, Y. Wu, P. Liu, B. S. Ong and R. A. Street, *Phys. Rev. B: Condens. Matter Mater. Phys.*, 2004, **70**, 115311.
- 45 P. Prins, F. C. Grozema, J. M. Schins, S. Patil, U. Scherf and L. D. A. Siebbeles, *Phys. Rev. Lett.*, 2006, **96**, 146601.
- 46 C. Scharsich, R. H. Lohwasser, M. Sommer, U. Asawapirom, U. Scherf, M. Thelakkat, D. Neher and A. Kohler, *J. Polym. Sci., Part B: Polym. Phys.*, 2012, **50**, 442–453.
- 47 K. Tashiro, M. Kobayashi, T. Kawai and K. Yoshino, *Polymer*, 1997, **38**, 2867–2879.
- 48 S. Gupta, Q. L. Zhang, T. Emrick and T. P. Russell, *Nano Lett.*, 2006, **6**, 2066–2069.
- 49 M. Zorn, M. N. Tahir, B. Bergmann, W. Tremel, C. Grigoriadis, G. Floudas and R. Zentel, *Macromol. Rapid Commun.*, 2010, **31**, 1101–1107.
- 50 M. Muthukumar, *Eur. Phys. J. E*, 2000, **3**, 199–202.
- 51 K. Zhao, L. J. Xue, J. G. Liu, X. Gao, S. P. Wu, Y. C. Han and Y. H. Geng, *Langmuir*, 2010, **26**, 471–477.
- 52 F. Binsberg, *Nature*, 1966, **211**, 516–517.
- 53 Y. K. Lan and C. I. Huang, *J. Phys. Chem. B*, 2009, **113**, 14555–14564.